

# A Numerical Study Comparing Adult Body, Head and Knee Coils for Paediatric MRI

Gemma R Cook<sup>1</sup>, Martin J Graves<sup>1</sup>, Owen J Arthurs<sup>2</sup>, Fraser J Robb<sup>3</sup>, and David J Lomas<sup>1</sup>

<sup>1</sup>Radiology, University of Cambridge, Cambridge, United Kingdom, <sup>2</sup>Great Ormond Street Hospital, London, United Kingdom, <sup>3</sup>GE Healthcare Coils, Aurora, OH, United States

**Target Audience:** Clinicians and physicists involved in radiofrequency paediatric coil selection and design.

**Purpose:** The limited availability of dedicated paediatric coils means that many centres typically perform paediatric MRI using a transmit/receive head or knee coil as they are considered to be more SAR and SNR advantageous. This study uses a FEM-compatible model of a two month old infant to determine the transmit ( $B_1^+$ ) and receive ( $B_1^-$ ) fields from birdcage designs with typical head and knee coil dimensions. Comparisons are made with a body coil.

**Methods:** Three quadrature coil representations – body coil (diameter: 72cm, length: 58cm), head coil (diameter: 28cm, length: 34cm), knee coil (diameter: 24cm, length: 20cm) – were designed and tuned to 64MHz using a commercially available FE solver (COMSOL Multiphysics, Stockholm, Sweden)<sup>1</sup>. These were then loaded by a FEM-compatible anatomical model of a three month old infant created in-house from manually segmented 3D post-mortem MR data. The tissue conductivity values were calculated according to their water content<sup>2</sup>. As patient position relative to the coil is known to alter loading and SAR<sup>3,4</sup> two physical positions of the model for each of the three coils (six simulations) were investigated. Maxwell's equations were solved to determine  $B_1^+$  and receive  $B_1^-$  fields and their uniformity was assessed within the entire patient volume and for smaller, more central volumes of interest, e.g. liver and heart, using fields scaled to 1 $\mu$ T at the isocentre.

Specific Absorption Rate (SAR) was normalised to a whole-body limit of 4W/kg<sup>4</sup> to determine local SAR (averaged over a 1cm<sup>3</sup> cube) at positions on a 3D grid. This SAR map was used as the heat source in the Pennes' Bio-Heat equation to estimate tissue temperature change accounting for blood perfusion, metabolic rate and skin emissivity.

**Results:** Figure 1 shows the  $B_1^+$  field uniformity in the three coils over the entire mode. Note that  $B_1^-$  is reciprocally uniform in the receive mode. Table 1 shows the relative  $B_1^+$  uniformity (calculated as  $B_{1^+MAX} - B_{1^+MIN}$  for the normalised field values) in the liver of the model for two different physical positions within the three coils. Figure 2 shows the normalised SAR for the three coils, with the maximum values reported in Table 1. Figure 3 shows the area of highest temperature change in the model's neck inside the body coil.

**Discussion:** The maximum SAR was at the narrowest point of the model inside the coil. For the body coil this was in the neck for both positions. However, when the models abdomen was centred in the knee and head coils the peak was found at the top of the leg, otherwise the maximum SAR was found in the neck. This is attributed to the increased current induced in narrower regions and the location of the maximum current within the model volume. The co-location of the SAR and temperature maxima results from a

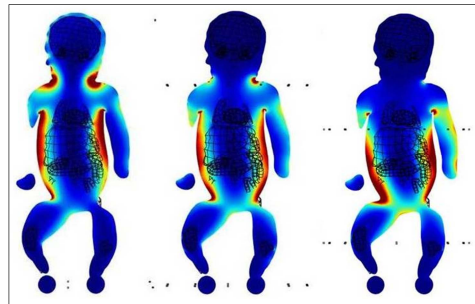


**Figure 2.** SAR maps for body, head and knee coils (L-R) from abdomen-centred simulations.

majority of the body being within the coil; lower maximum temperature changes occur when blood flow distributes heat into cooler regions, further peak SAR values.

The birdcage design produces uniform  $B_1^+$  fields within the end rings. Within the liver (and other organs), however, relative  $B_1^+$  uniformity and non-scaled  $B_1^+$  values are increased with a small coil diameter. Organ-specific imaging would therefore benefit from the smallest coil that can fit the organ inside its field of view though other results raise concern over the SAR cost.

Temperature and peak SAR are reduced by having less of the model within the coil; this suggests a benefit to using local transmit coils, however, this rule was counteracted if the baby is arranged with its neck in areas of high electric field.

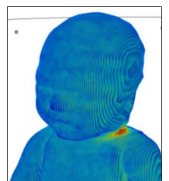


**Figure 3.**  $\Delta T$  for head (body coil)

Coil	Isocentre Position	Relative $B_1^+$ uniformity in the Liver	Max. SAR (W/kg)	Max. $\Delta T$ (K)
Body	Chest	0.54	67.37	0.40
	Abdomen	0.56	54.52	0.31
Head	Chest	0.43	62.91	0.37
	Abdomen	0.39	29.25	0.16
Knee	Chest	0.32	73.92	0.34
	Abdomen	0.61	51.84	0.19

**Table 1:** Numerical comparison of measures of field homogeneity in the liver, SAR and induced temperature change.

**Conclusion:** Though the selection of coil for signal reception appears obvious from the receive field uniformity, the transmit coil selection is more complex. The SAR maps indicate that local limits are exceeded in the worst-case scenario with all the coils, though the SAR maximum is significantly reduced when the child is partially removed from the  $B_1^+/B_1^-$  homogeneous region. SAR and temperature change cannot be analysed in isolation from one another, especially when the infant is only partially exposed to RF.

**References:** 1. Gurler et al. Proc. COMSOL Conference, Milan (2012) 2. Wang et al. IEEE Trans. on Electromagnetic Compatibility 48(2):408-413 (2006) 3. Collins et al. Magn. Reson. Med. 65:1470-1482 (2011) 4. Murbach et al. Prog. Biophys Mol Biol. 107(3): 428-33 (2011)